

***Supplementary Information for
Synthesis of the Seismic Structure of the Greater
Alaska Region: Continental Lithosphere***

**Xiaotao Yang¹, Michael Everett Mann², Karen Fischer², Margarete
Jadamec^{3,4}, S. Shawn Wei⁵, Gary Pavlis⁶, and Andrew Schaeffer⁷**

¹Department of Earth, Atmospheric, and Planetary Sciences, Purdue University, West Lafayette, IN,
USA.

²Department of Earth, Environmental, and Planetary Sciences, Brown University, Providence, Rhode
Island, USA.

³Department of Geology, University at Buffalo, SUNY, Buffalo, New York, USA.

⁴Institute for Artificial Intelligence and Data Science, University at Buffalo, SUNY, Buffalo, New York,
USA.

⁵Department of Earth and Environmental Sciences, Michigan State University, East Lansing, MI, USA.

⁶Department of Earth and Atmospheric Sciences, Indiana University Bloomington, Bloomington, IN,
USA.

⁷Geological Survey of Canada Pacific Division, Sidney Subdivision, Natural Resources Canada, Sidney,
BC, CA.

Contents in this file

Supplementary Figures S1-S10.

Supplementary Table S1

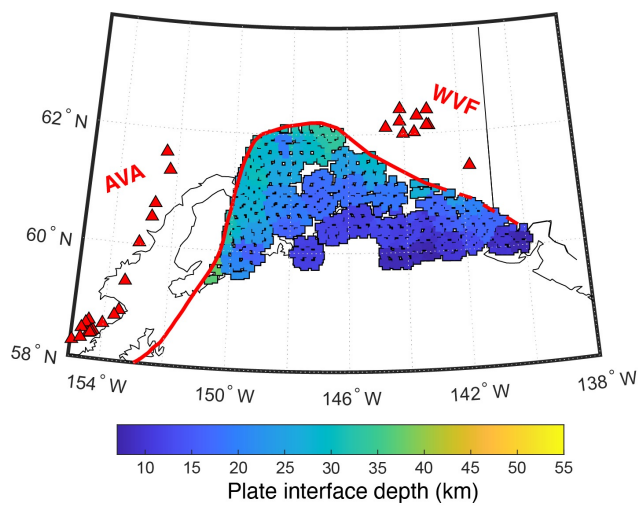


Figure S1. Plate interface depth from Mann et al. (2022) that is used as the thickness of the overriding crust south of the intersection between the plate interface and the overriding Moho, termed Plate Interface Extent (PIE, the thick red line). The PIE Line is dashed at the eastern end where it is unclear if the subducting slab reaches the overriding mantle (Mann et al., 2022). Red triangles are active arc volcanoes. WVF – Wrangell Volcanic Field. AVA – Aleutian Volcanic Arc.

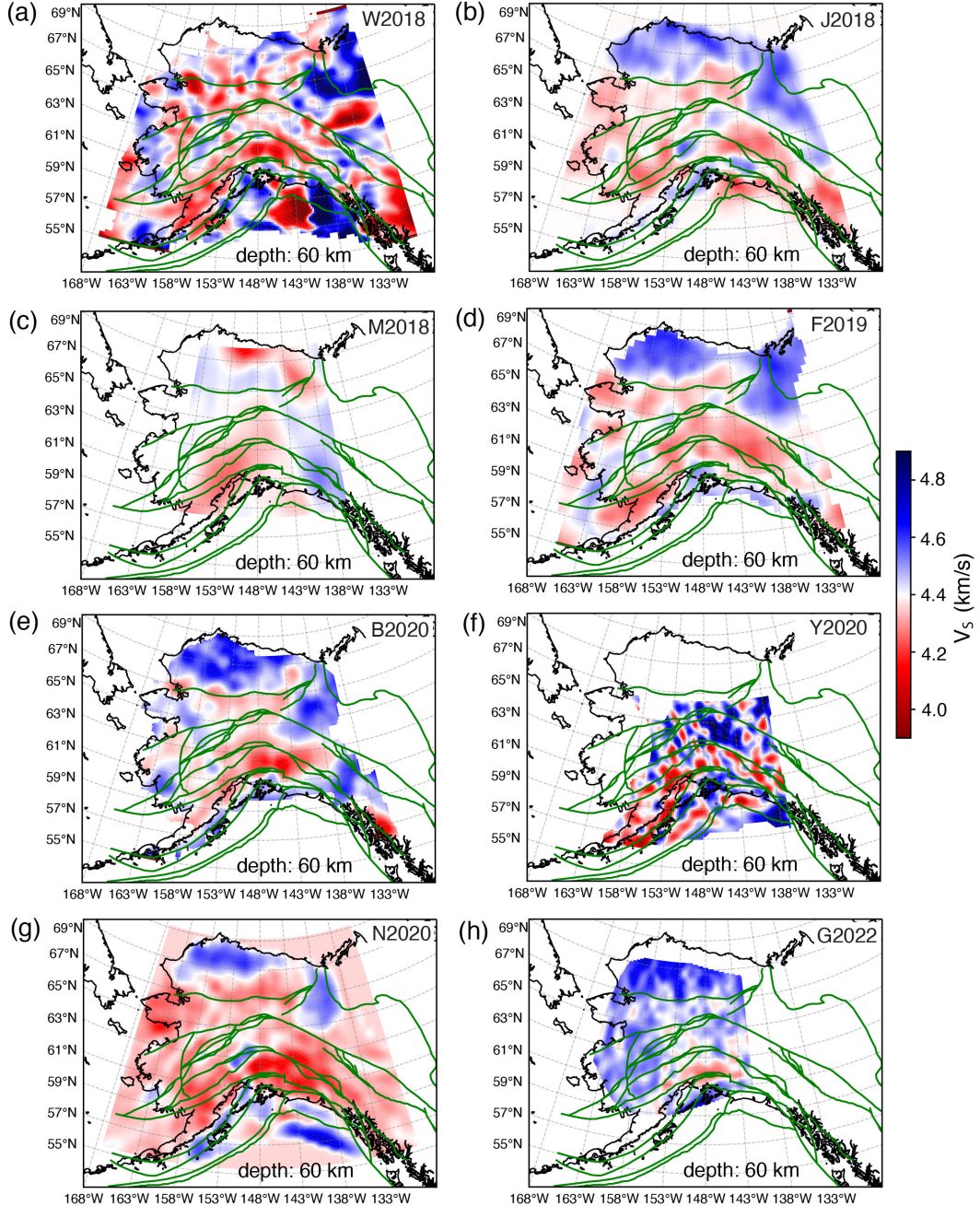


Figure S2. Examples of the shear-wave velocity models at the depth of 60 km for all models. (a-h) Depth slices from models W2018 (Ward & Lin, 2018), J2018 (Jiang et al., 2018), M2018 (Martin-Short et al., 2018), F2019 (Feng & Ritzwoller, 2019), B2020 (Berg et al., 2020), Y2020 (Yang & Gao, 2020), N2020 (Nayak et al., 2020), and G2022 (Gama et al., 2022b). Major faults (thick green lines) are shown for reference. After interpolations onto 0.2 (longitudes) by 0.1 (latitudes) grids, we smooth all models laterally over five grids for plotting.

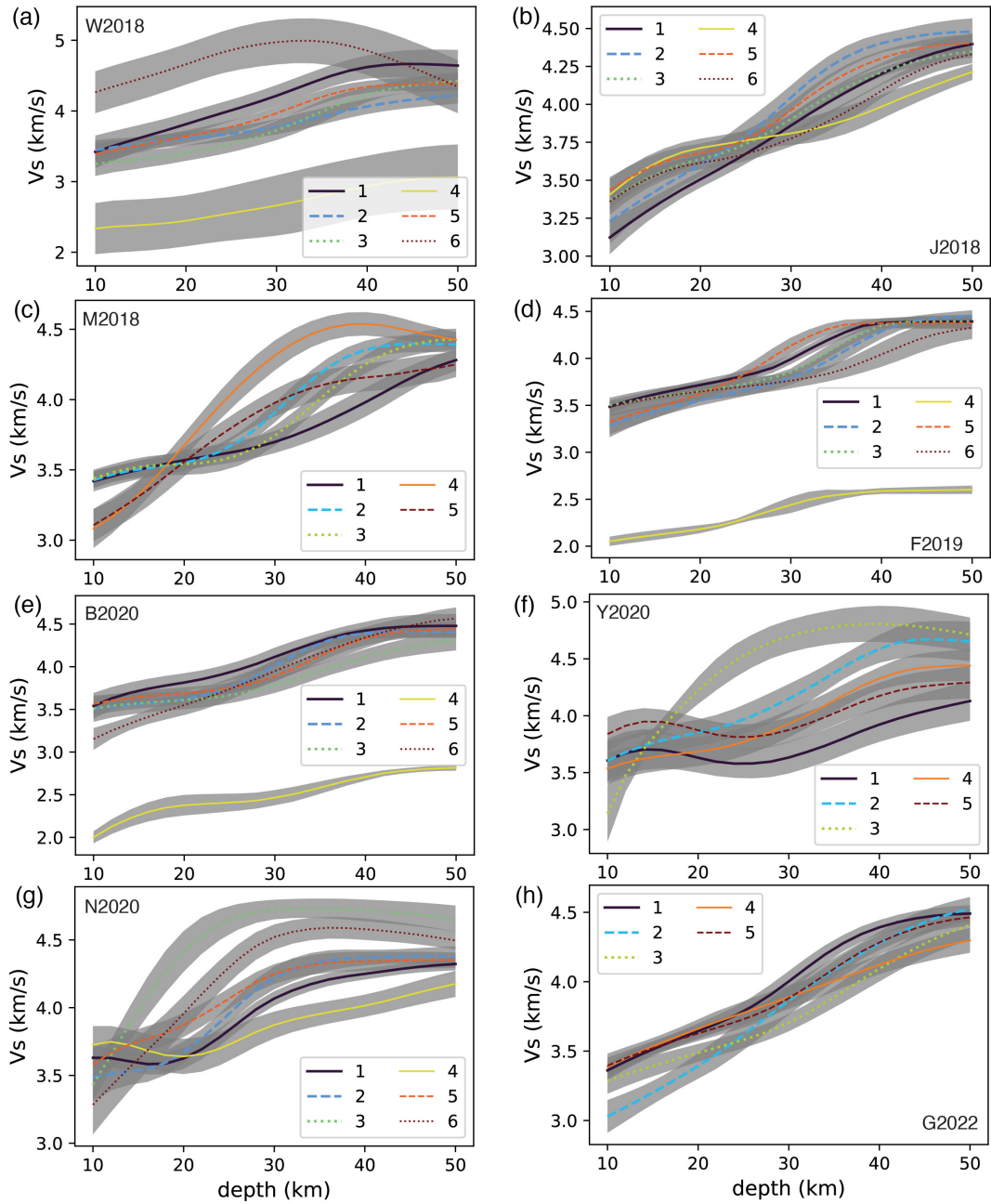


Figure S3. Centers of velocity clusters for all velocity models at the depths of 10–50 km. The model label is shown for each pane. The shaded gray area denotes the 68% confidence interval around the cluster center defined as one standard deviation from the center.

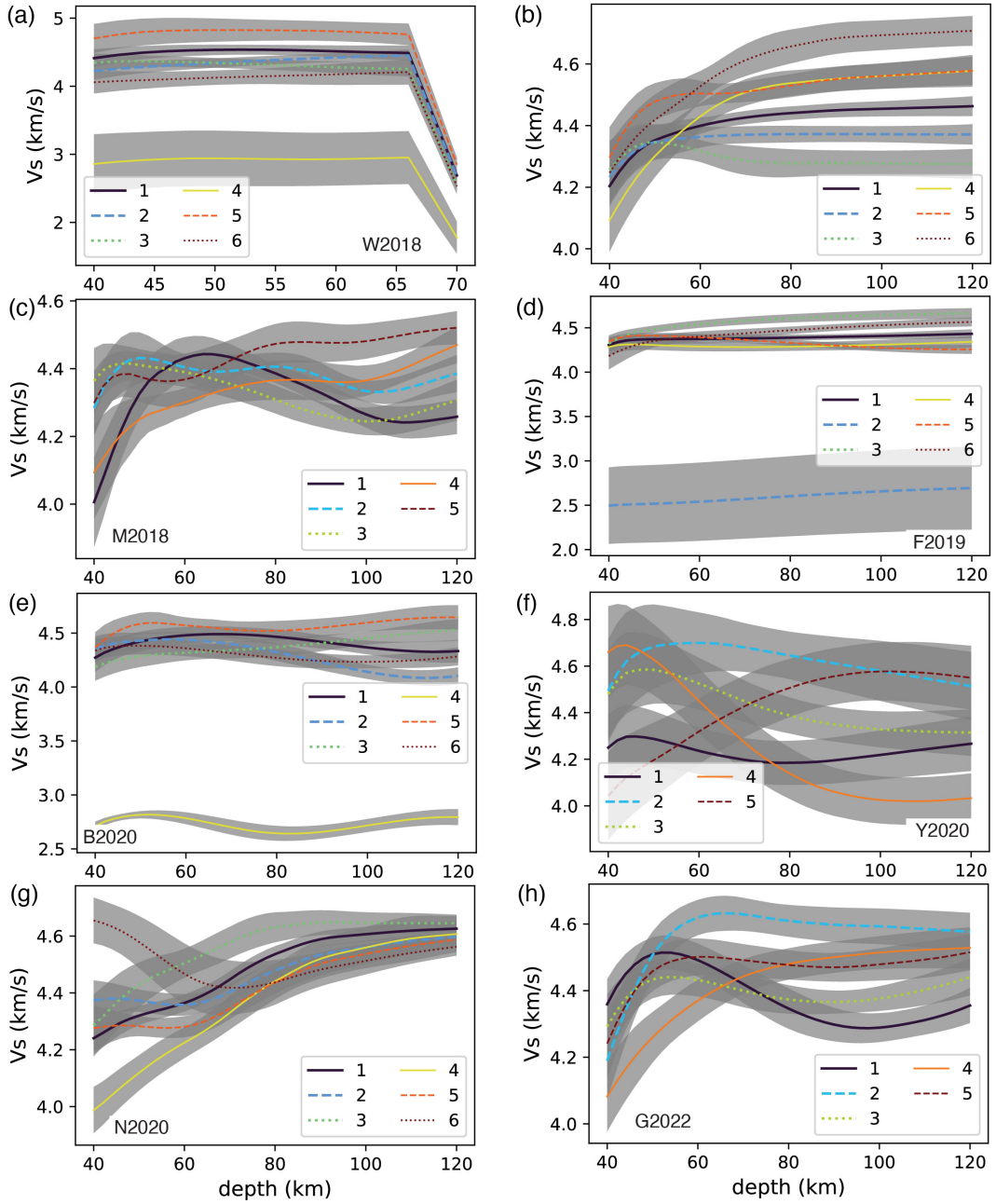


Figure S4. Centers of velocity clusters for all velocity models at the depths of 40-120 km. The model label is shown for each pane. The shaded gray area denotes the 68% confidence interval around the cluster center defined as one standard deviation from the center. Note that W2018 (panel a) only covers the depth down to 70 km.

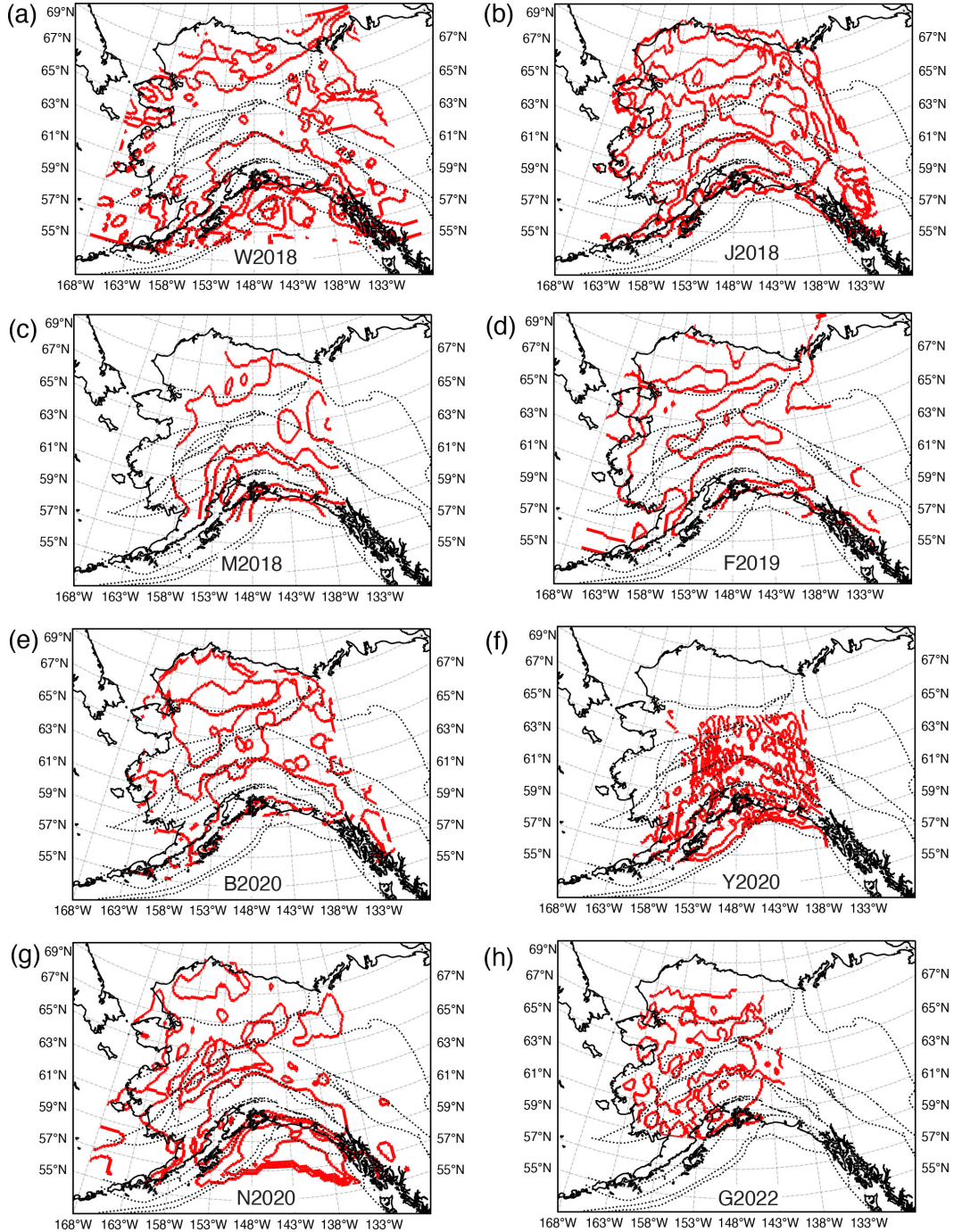


Figure S5. Detected cluster boundaries (red pixels) for velocities at the depths of 10–50 km. The dotted lines are major fault lines as in Figure 1b in the main text.

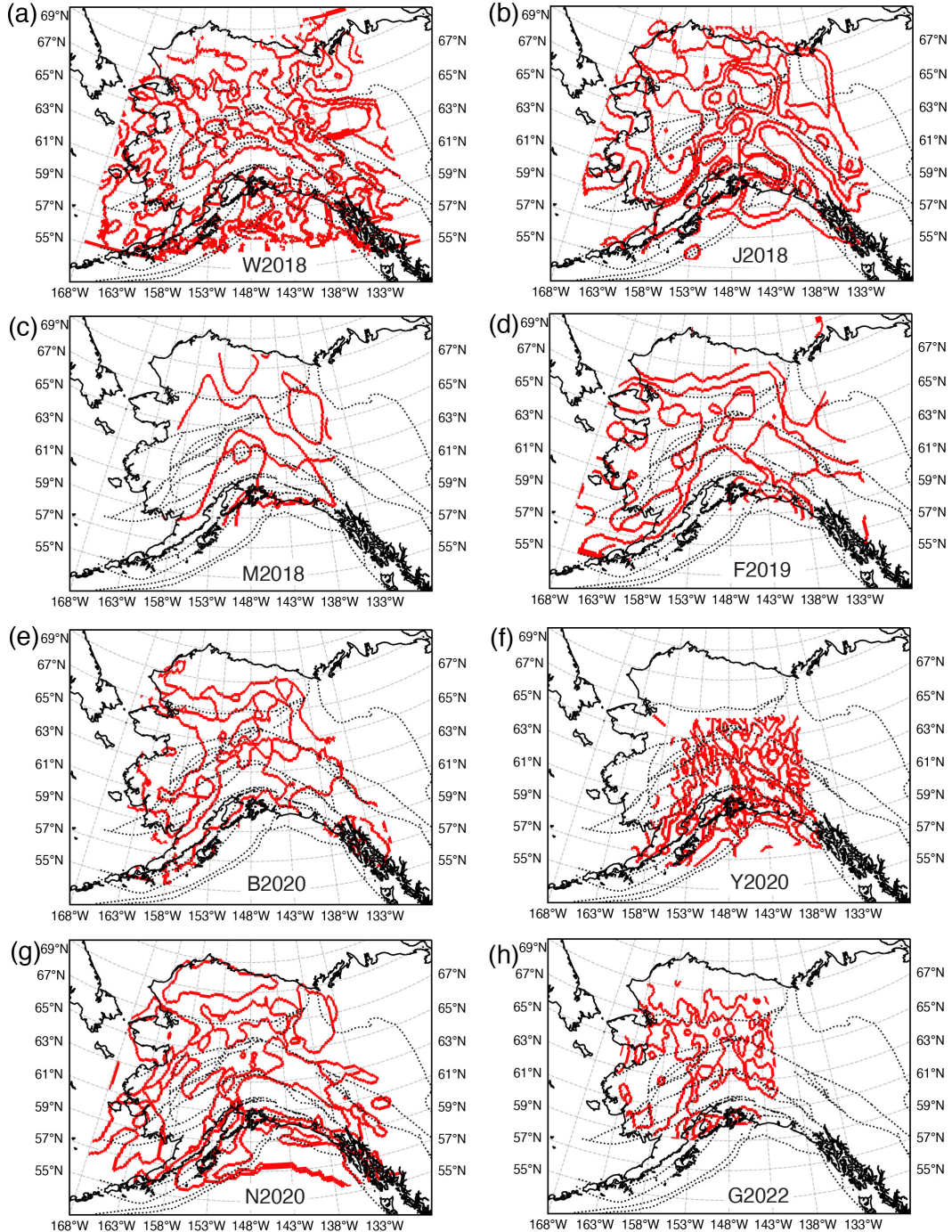


Figure S6. Detected cluster boundaries (red pixels) for velocities at the depths of 40-120 km. The dotted lines are major fault lines as in Figure 1b in the main text.

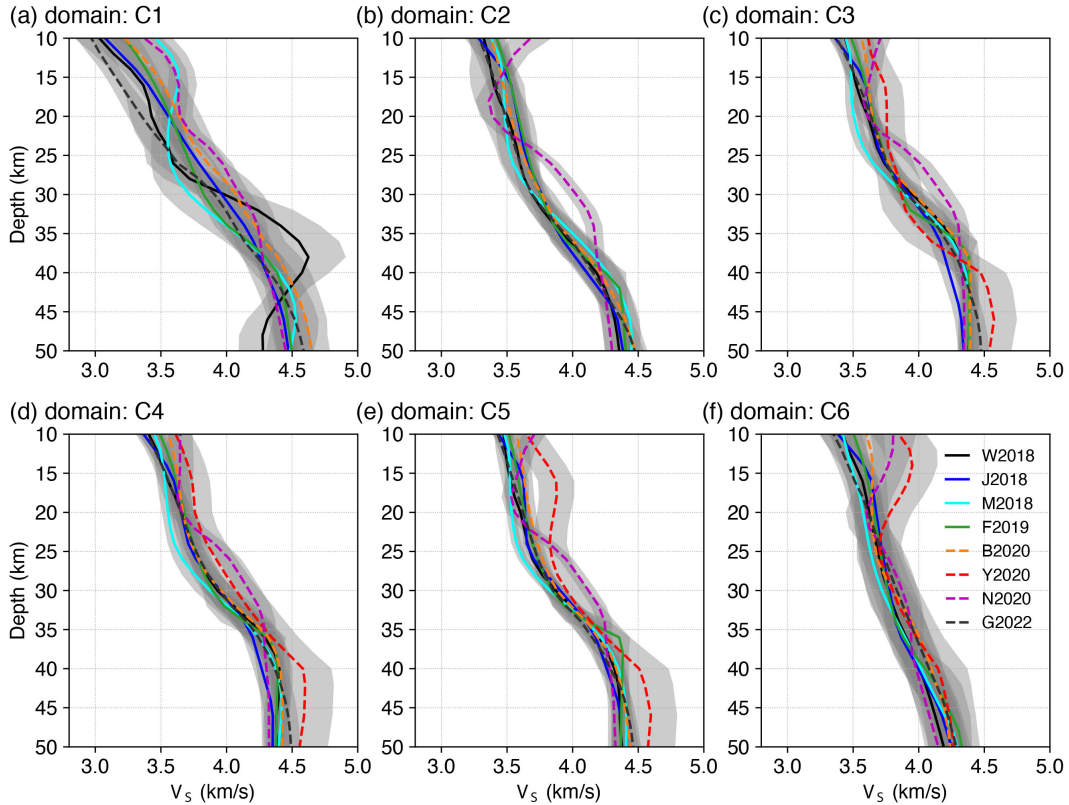


Figure S7. Average velocity profiles within the identified structural domains at the depths of 10–50 km as in Figure 10a in the main text. (a-f) The profiles color-coded by velocity models. The gray shaded area for each profile shows the range of one standard deviation below and above the average velocity profile.

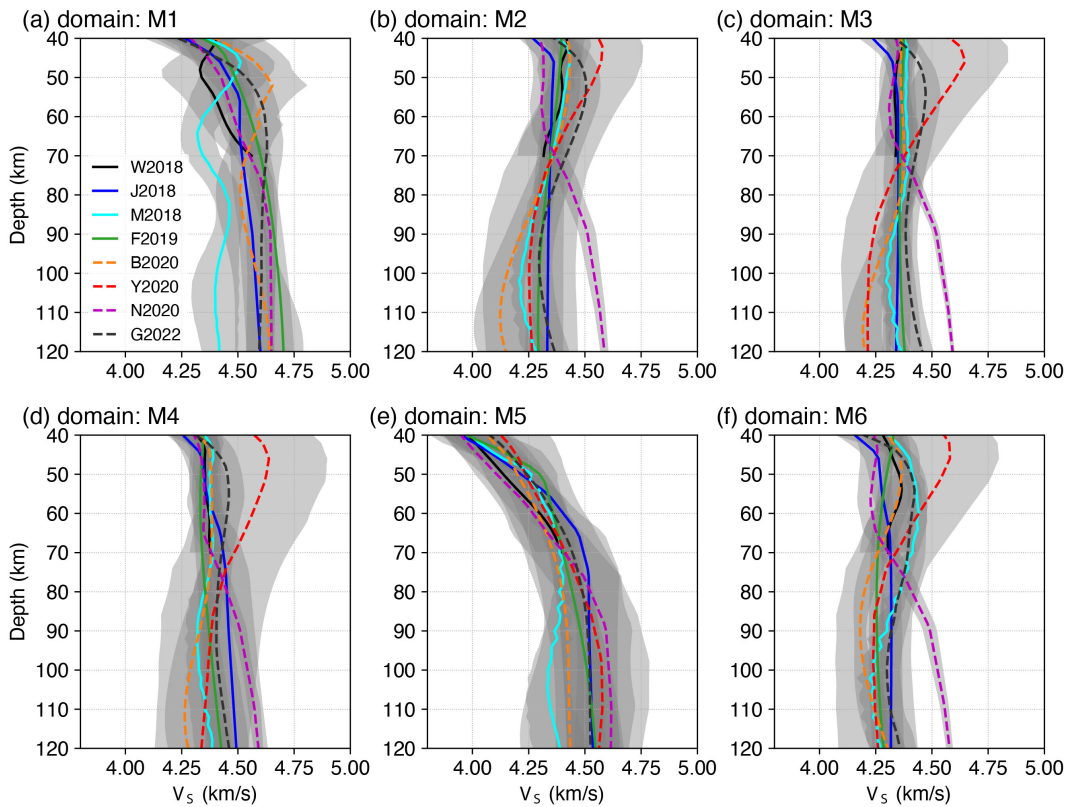


Figure S8. Same as Figure S7 but for the identified structural domains at the depths of 40–120 km as in Figure 10b in the main text. Note that W2018 (black solid line) only covers the depth down to 70 km.

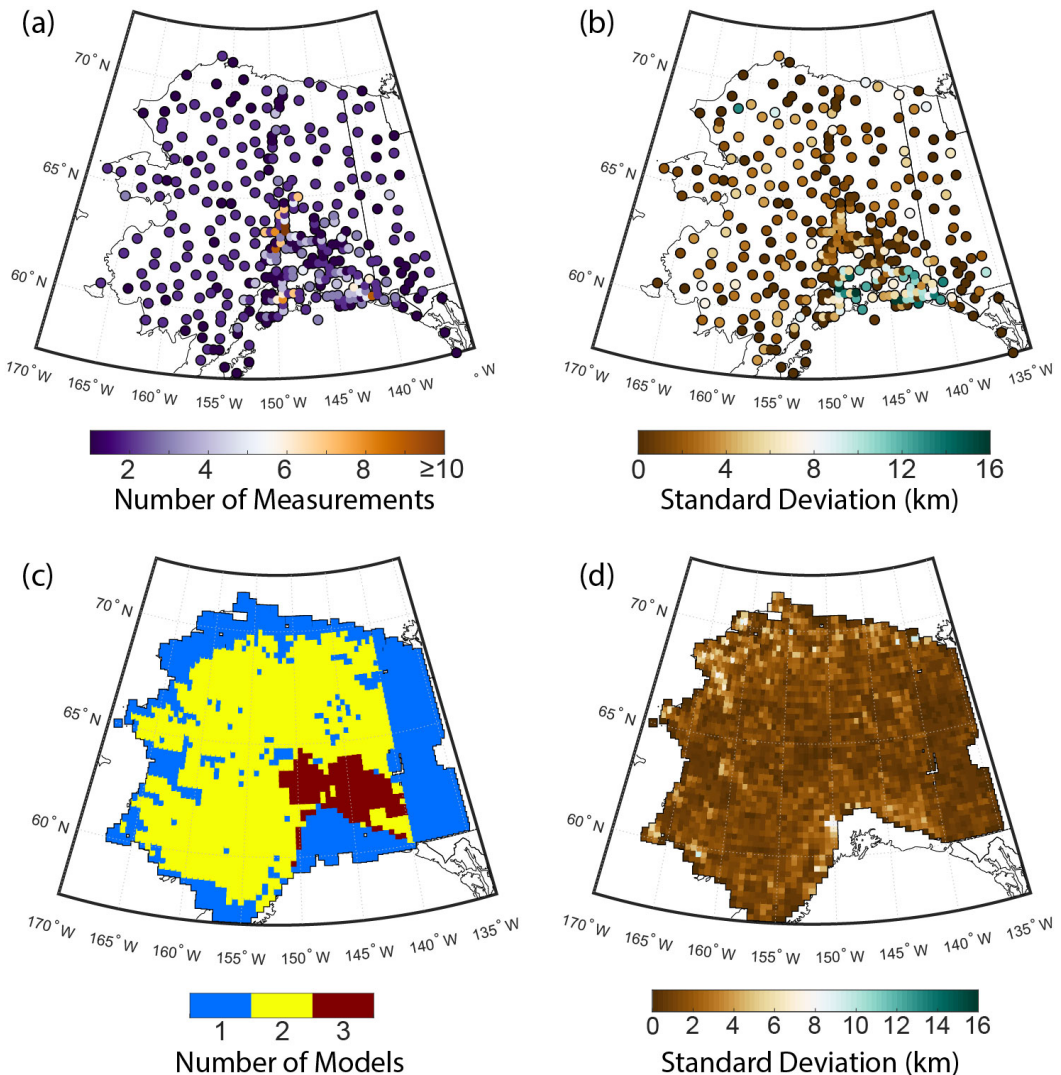


Figure S9. Number of measurements (left) and standard deviations (right) when averaging the crustal thickness models. (a-b) For single-station estimates. The Broadband Experiment Across Alaskan Range stations in south-central Alaska were deployed in dense clusters with several stations at one site, resulting in multiple measurements for one site on the map. (c-d) For multi-station models.

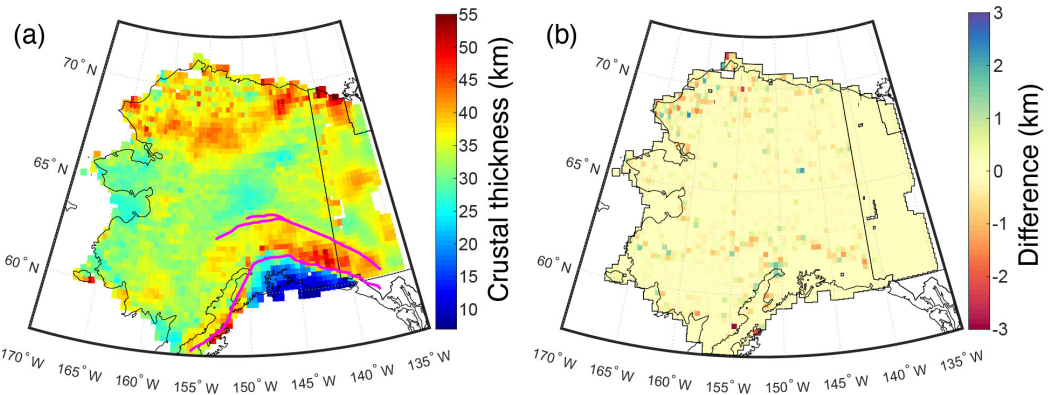


Figure S10. Average crustal thicknesses from the multi-station studies including uncertainties. (a) Average of multi-station crustal thicknesses within each 0.5° (longitude) by 0.25° (latitude) bin, using uncertainties as inverse weights in the two-step averaging (averaging of values in a bin for a given study, and then averaging of values in a bin between studies). To the south of the Plate Interface Extent (PIE) line, the map is showing the depth to the top of the subducting plate. (b) The difference between multi-station crustal thicknesses obtained with uncertainties in the input data (a) and crustal thicknesses obtained without using uncertainties as weights (Figure 11b in the main text). The difference is computed as $d_0 - d_u$, where d_0 is the Moho in Figure 11b in the main text and d_u is the Moho in (a) with uncertainties considered.

Table S1: Seismic network information from the International Federation of Digital Seismograph Networks.

Code	Description	Reference
5C	Dynamics of Lake-Calving Glaciers: Yakutat Glacier, Alaska	Martin Truffer. (2009). Dynamics of Lake-Calving Glaciers: Yakutat Glacier, Alaska. International Federation of Digital Seismograph Networks. https://doi.org/10.7914/SN/5C_2009
7C	The Mackenzie Mountains Transect: Active Deformation from Margin to Craton	Derek Schutt & Rick Aster. (2015). The Mackenzie Mountains Transect: Active Deformation from Margin to Craton. International Federation of Digital Seismograph Networks. https://doi.org/10.7914/SN/7C_2015
AK	Alaska Regional Network	Alaska Earthquake Center & Univ. of Alaska Fairbanks. (1987). Alaska Regional Network [Data set]. International Federation of Digital Seismograph Networks. https://doi.org/10.7914/SN/AK
AT	National Tsunami Warning System	NOAA National Oceanic and Atmospheric Administration (USA). (1967). National Tsunami Warning Center Alaska Seismic Network [Data set]. International Federation of Digital Seismograph Networks. https://doi.org/10.7914/SN/AT
AV	Alaska Volcano Observatory	Alaska Volcano Observatory/USGS. (1988). Alaska Volcano Observatory [Data set]. International Federation of Digital Seismograph Networks. https://doi.org/10.7914/SN/AV
CN	Canadian National Seismograph Network	Natural Resources Canada (NRCan Canada). (1975). Canadian National Seismograph Network [Data set]. International Federation of Digital Seismograph Networks. https://doi.org/10.7914/SN/CN
II	Global Seismograph Network (GSN-IRIS/IDA)	Scripps Institution of Oceanography. (1986). Global Seismograph Network - IRIS/IDA [Data set]. International Federation of Digital Seismograph Networks. https://doi.org/10.7914/SN/II
IM	International Miscellaneous Stations (IMS)	-
IU	Global Seismograph Network (GSN-IRIS/USGS)	Albuquerque Seismological Laboratory/USGS. (2014). Global Seismograph Network (GSN - IRIS/USGS) [Data set]. International Federation of Digital Seismograph Networks. https://doi.org/10.7914/SN/IU
PP	Princeton Earth Physics Program	-
PQ	Public Safety Geoscience Program Canadian Research Network	Geological Survey of Canada. (2013). Public Safety Geoscience Program Canadian Research Network [Data set]. International Federation of Digital Seismograph Networks. https://doi.org/10.7914/SN/PQ
TA	USArray Transportable Array	IRIS Transportable Array. (2003). USArray Transportable Array [Data set]. International Federation of Digital Seismograph Networks. https://doi.org/10.7914/SN/TA

Continued on next page

Table S1 – continued from previous page

Code	Description	Reference
US	United States National Seismic Network	Albuquerque Seismological Laboratory (ASL)/USGS. (1990). United States National Seismic Network [Data set]. International Federation of Digital Seismograph Networks. https://doi.org/10.7914/SN/US
XE	Broadband Experiment Across Alaskan Range (BEAAR)	Douglas Christensen, Roger Hansen & Geoff Abers. (1999). Broadband Experiment Across the Alaska Range [Data set]. International Federation of Digital Seismograph Networks. https://doi.org/10.7914/SN/XE_1999
XF	Relating glacier-generated seismicity to ice motion, basal processes and iceberg calving	Chris Larsen & Michael West. (2009). Collaborative Research: Relating glacier-generated seismicity to ice motion, basal processes and iceberg calving. [Data set]. International Federation of Digital Seismograph Networks. https://doi.org/10.7914/SN/XF_2009
XL	Dynamic controls on tidewater glacier retreat	Shad O'Neil. (2008). Collaborative Research: Dynamic controls on tidewater glacier retreat [Data set]. International Federation of Digital Seismograph Networks. https://doi.org/10.7914/SN/XL_2008
XM	Broadband recording at the site of great earthquake rupture in the Alaska Megathrust	Katie Kieranen. (2011). Broadband recording at the site of great earthquake rupture in the Alaska Megathrust [Data set]. International Federation of Digital Seismograph Networks. https://doi.org/10.7914/SN/XM_2011
XN	Canadian Northwest Experiment	Jim Gaherty & Justin Revenaugh. (2003). Collaborative Research: Canadian Northwest Seismic Experiment [Data set]. International Federation of Digital Seismograph Networks. https://doi.org/10.7914/SN/XN_2003
XO	Alaska Amphibious Community seismic Experiment (AACSE)	Geoff Abers, Douglas Wiens, Susan Schwartz, Anne Sheehan, Donna Shillington, Lindsay Worthington, Patrick Shore, Emily Rowland, Spahr Webb & Aubreya Adams. (2018). AACSE: Alaska Amphibious Community seismic Experiment [Data set]. International Federation of Digital Seismograph Networks. https://doi.org/10.7914/SN/XO_2018
XR	Observational and Theoretical Constraints on the Structure and Rotation of the Inner Core (ARTIC)	Xiaodong Song & Douglas Christensen. (2004). CSEDI: Observational and Theoretical Constraints on the Structure and Rotation of the Inner Core [Data set]. International Federation of Digital Seismograph Networks. https://doi.org/10.7914/SN/XR_2004
XV	Fault Locations and Alaska Tectonics from Seismicity (FLATS)	Carl Tape & Michael E. West. (2014). Fault Locations and Alaska Tectonics from Seismicity [Data set]. International Federation of Digital Seismograph Networks. https://doi.org/10.7914/SN/XV_2014
XZ	St. Elias Erosion and Tectonics Project (STEEP)	Roger Hansen & Gary Pavlis. (2005). Collaborative Research: St. Elias Erosion/Tectonics Project [Data set]. International Federation of Digital Seismograph Networks. https://doi.org/10.7914/SN/XZ_2005

Continued on next page

Table S1 – continued from previous page

Code	Description	Reference
YE	Bench Glacier Seismic Network	John Bradford. (2007). Water storage and routing within glaciers via planar voids, a new model of glacier hydrology [Data set]. International Federation of Digital Seismograph Networks. https://doi.org/10.7914/SN/YE_2007
YG	Wrangell Volcanism and Lithospheric Fate (WVLF) experiment	Douglas Christensen & Geoff Abers. (2016). Fate and consequences of Yakutat terrane subduction beneath eastern Alaska and the Wrangell Volcanic Field [Data set]. International Federation of Digital Seismograph Networks. https://doi.org/10.7914/SN/YG_2016
YM	Denali Fault Aftershocks RAMP	Roger Hansen. (2002). Denali Fault Aftershocks RAMP [Data set]. International Federation of Digital Seismograph Networks. https://doi.org/10.7914/SN/YM_2002
YO	Tidewater glacier and ice marginal dynamic behavior	Dan Lawson, Shad O’Neel, Gordon Hamilton, Leigh Stearns & David Finnegan (2010): Tidewater glacier and ice marginal dynamic behavior. International Federation of Digital Seismograph Networks. Other/Seismic Network. https://doi.org/10.7914/SN/YO_2010
YV	Multidisciplinary Observations of Subduction (MOOS)	Geoffrey Abers & Douglas Christensen (2006): Multidisciplinary Observations Of Subduction. International Federation of Digital Seismograph Networks. Other/Seismic Network. https://doi.org/10.7914/SN/YV_2006
Z5	A four-dimensional view of deformation in the Eastern Alaska Range - where did the slip on the Denali fault go? (ICED)	Meghan S. Miller, Sarah M. Roeske, Jeff A & Benowitz. (2018). A four-dimensional view of deformation in the Eastern Alaska Range - where did the slip on the Denali fault go? [Data set]. International Federation of Digital Seismograph Networks. https://doi.org/10.7914/SN/Z5_2018
ZE	Southern Alaska Lithosphere and Mantle Observation Network (SALMON)	Carl Tape, Douglas H. Christensen & Melissa M. Moore-Driskell. (2015). Southern Alaska Lithosphere and Mantle Observation Network [Data set]. International Federation of Digital Seismograph Networks. https://doi.org/10.7914/SN/ZE_2015

References

- Berg, E. M., Lin, F. C., Allam, A., Schulte-Pelkum, V., Ward, K. M., & Shen, W. (2020, 2). Shear velocity model of Alaska via joint inversion of rayleigh wave ellipticity, phase velocities, and receiver functions across the Alaska transportable array. *Journal of Geophysical Research: Solid Earth*, 125, e2019JB018582. Retrieved from <https://onlinelibrary.wiley.com/doi/full/10.1029/2019JB018582> doi: 10.1029/2019JB018582
- Feng, L., & Ritzwoller, M. H. (2019). A 3-D shear velocity model of the crust and uppermost mantle beneath Alaska including apparent radial anisotropy. *Journal of Geophysical Research: Solid Earth*, 124, 10468-10497. doi: 10.1029/2019JB018122
- Gama, I., Fischer, K. M., Dalton, C. A., & Eilon, Z. (2022b, 12). Variations in Lithospheric Thickness across the Denali Fault and in Northern Alaska. *Geophysical Research Letters*, e2022GL101256. Retrieved from <https://onlinelibrary.wiley.com/doi/full/10.1029/2022GL101256> doi: 10.1029/2022GL101256
- Jiang, C., Schmandt, B., Ward, K. M., Lin, F., & Worthington, L. L. (2018, 10). Upper mantle seismic structure of Alaska from Rayleigh and S wave tomography. *Geophysical Research Letters*, 45, 10,350-10,359. Retrieved from <https://onlinelibrary.wiley.com/doi/10.1029/2018GL079406> doi: 10.1029/2018GL079406
- Mann, M. E., Abers, G. A., Daly, K. A., & Christensen, D. H. (2022, 1). Subduction of an oceanic plateau across southcentral Alaska: Scattered-wave imaging. *Journal of Geophysical Research: Solid Earth*, 127. doi: 10.1029/2021JB022697
- Martin-Short, R., Allen, R., Bastow, I. D., Porritt, R. W., & Miller, M. S. (2018, 11). Seismic imaging of the Alaska subduction zone: Implications for slab geometry and volcanism. *Geochemistry, Geophysics, Geosystems*, 19, 4541-4560. Retrieved from <https://onlinelibrary.wiley.com/doi/10.1029/2018GC007962> doi: 10.1029/2018GC007962
- Nayak, A., Eberhart-Phillips, D., Ruppert, N. A., Fang, H., Moore, M. M., Tape, C., ... Thurber, C. H. (2020, 11). 3D seismic velocity models for Alaska from joint tomographic inversion of body-wave and surface-wave data. *Seismological Research Letters*, 91, 3106-3119. Retrieved from <http://pubs.geoscienceworld.org/ssa/srl/article-pdf/91/6/3106/5176960/srl-2020214.1.pdf> doi: 10.1785/0220200214
- Ward, K. M., & Lin, F. C. (2018). Lithospheric structure across the Alaskan cordillera from the joint inversion of surface waves and receiver functions. *Journal of Geophysical Research: Solid Earth*, 123, 8780-8797. doi: 10.1029/2018JB015967
- Yang, X., & Gao, H. (2020, 11). Segmentation of the Aleutian-Alaska subduction zone revealed by full-wave ambient noise tomography: Implications for the along-strike variation of volcanism. *Journal of Geophysical Research: Solid Earth*, 125, 1-20. Retrieved from <https://onlinelibrary.wiley.com/doi/10.1029/2020JB019677> doi: 10.1029/2020JB019677